



Children's Hospital
Informatics Program

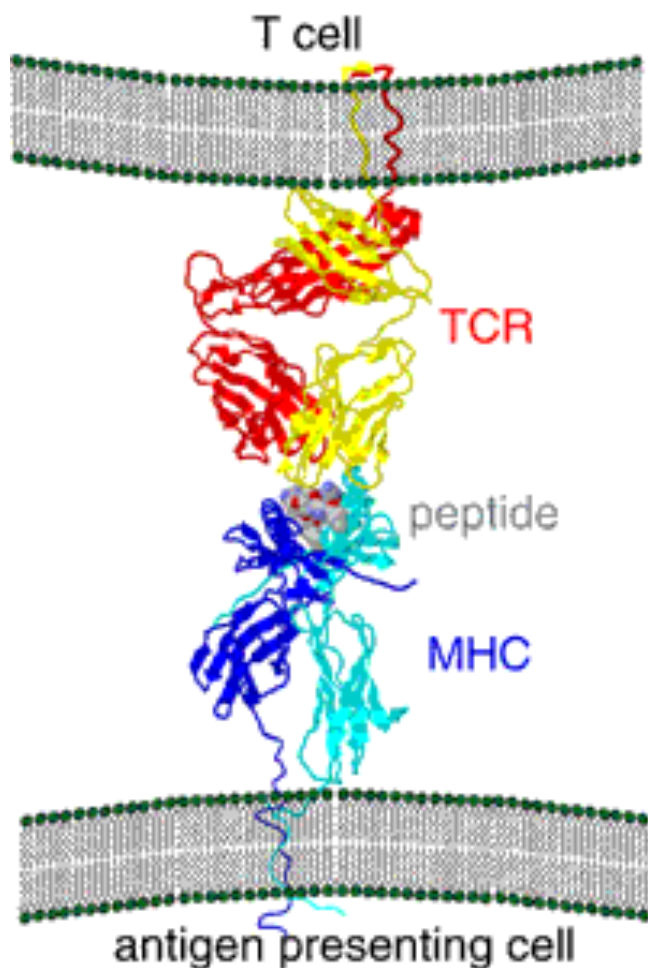


Harvard
Medical School

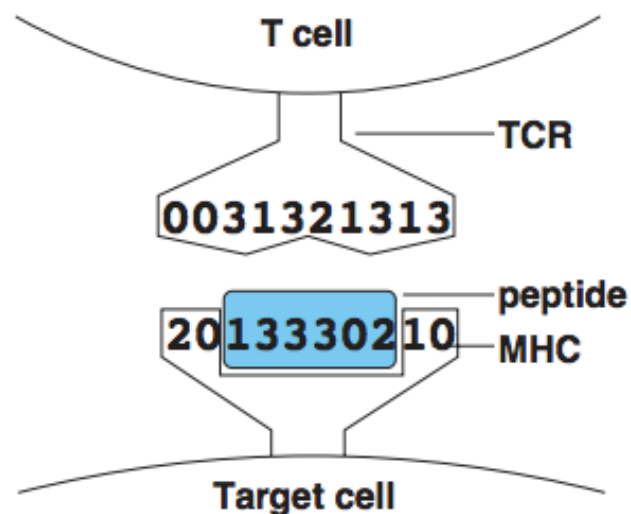


Using large repositories of SNP data for cancer immunotherapy and biomarker development

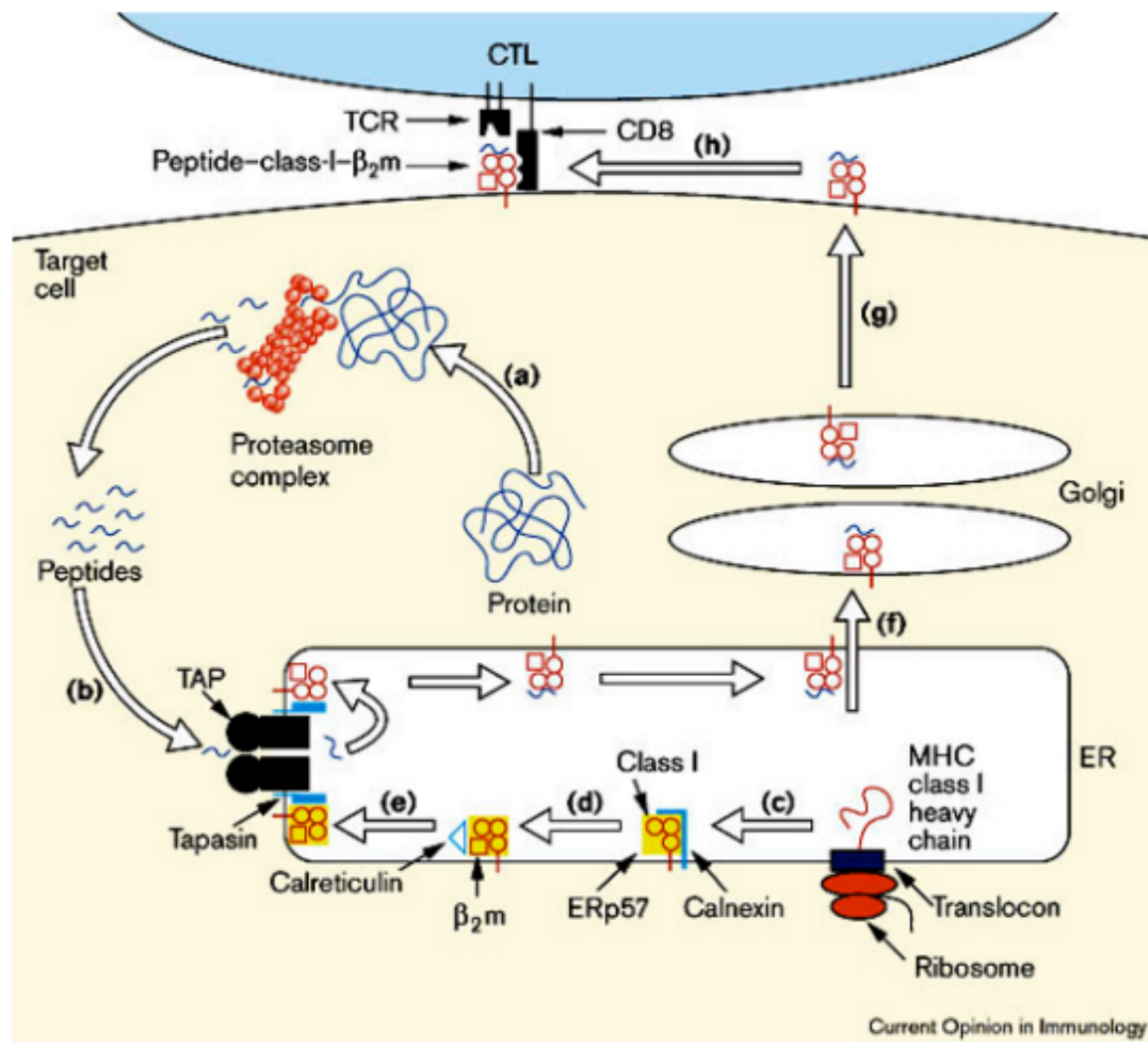
Russell Hanson

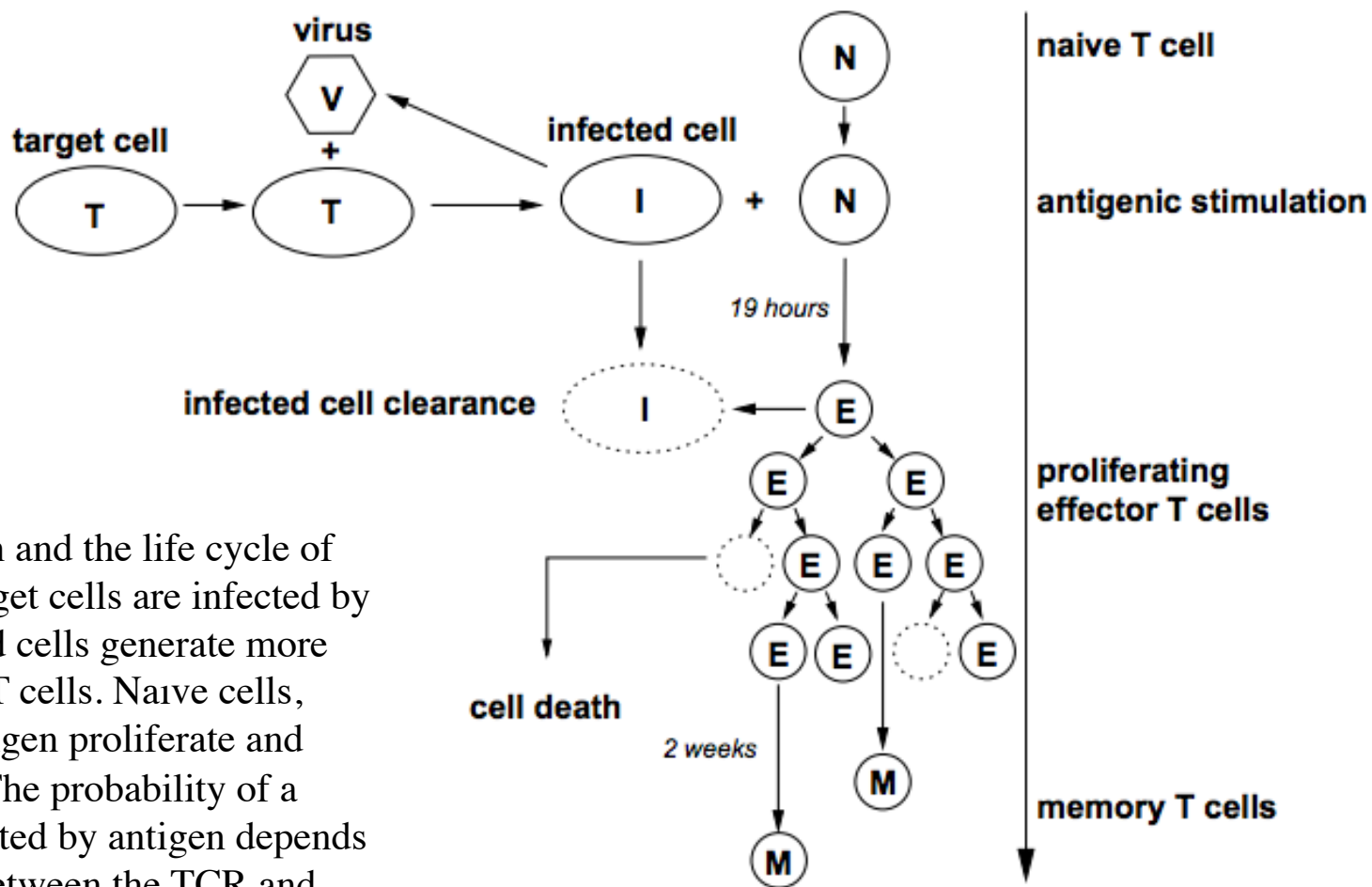


Cytotoxic T lymphocytes (CTL) play a central role in defeating intracellular infections with pathogens, such as viruses and certain bacteria. The CTL T-cell receptor (TCR) recognizes foreign peptides in complex with major histocompatibility complex (MHC) class I molecules on the surface of the infected cells. MHC class I molecules preferably bind and present nine amino acid long peptides, which mainly originates from proteins expressed in the cytosol of the presenting cell. In most mammals, MHCs exist in a number of different allelic variants each of which binds to a specific and very limited set of peptides.



Peptide generation in the class I pathway





The process of infection and the life cycle of CTLs in the model. Target cells are infected by virus, and these infected cells generate more virus and interact with T cells. Naive cells, when stimulated by antigen proliferate and become effector cells. The probability of a naive cell being stimulated by antigen depends on the string distance between the TCR and the antigen-MHC complex. Most effectors die, but about 5% of these proliferating effector cells become memory cells. The memory cells can be stimulated to become effectors in a secondary response (not shown).

Immune escape

- Pathogens evolve under *strong* selection pressure to avoid CTL recognition
- Generate point mutations or insertions/deletions to disturb
 - Peptide binding to MHC
 - CTL recognition
 - Only involve the antigenic peptide region
 - Antigen processing
 - Can involve peptide flanking region

Use Artificial Neural Networks (ANN) to predict MHC-I binding affinities

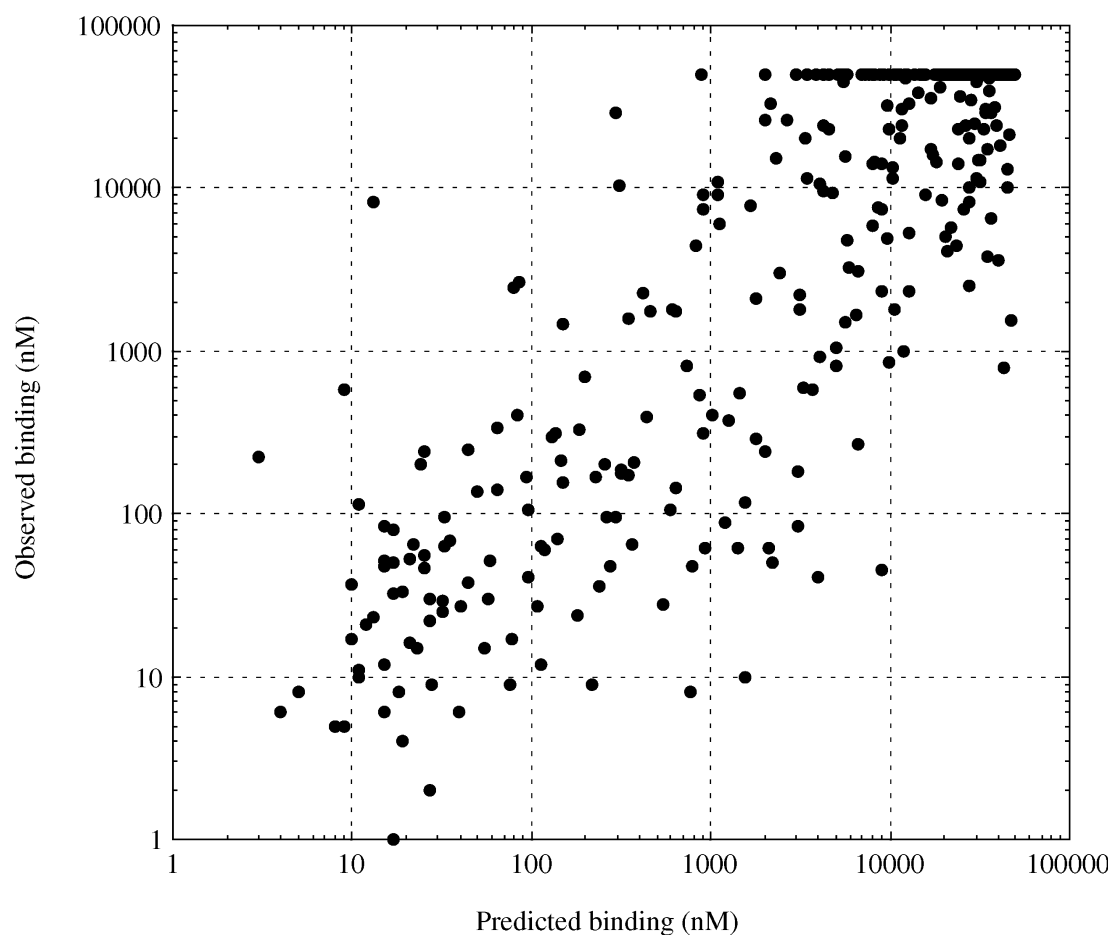
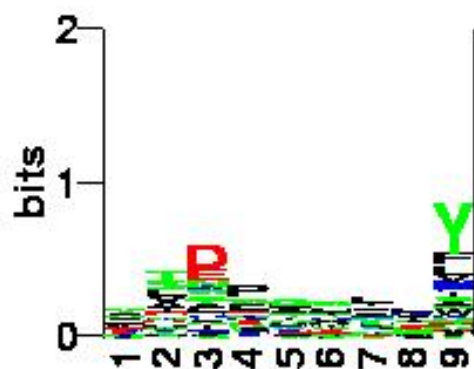
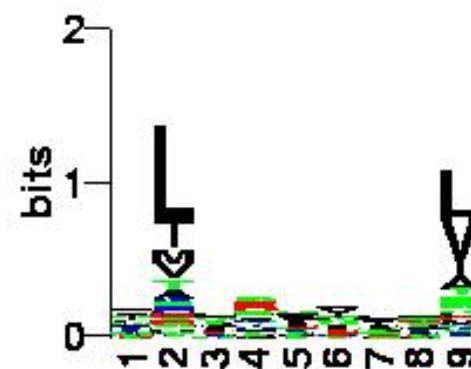


Fig. 1. ANN can perform quantitative predictions of peptide–MHC–I interaction. The binding affinity was measured in a biochemical assay (31) and expressed as the logarithm of the equilibrium dissociation constant (K_D (nM)). Subsequently, first generation ANN were trained to quantitatively predict the logarithm of the affinity of peptide binding to HLA-A*0204 using a cross-validation approach. This allowed the affinity of every peptide to be predicted by an ANN, which had not been trained on the peptide in question. The logarithm of the predicted binding *vs* the logarithm of the observed binding was plotted and analyzed by linear regression. The regression line was $y = 0.99x - 0.02$ ($n = 397$, $C_{\text{Pearson}} = 0.87$, $P < 0.001$).

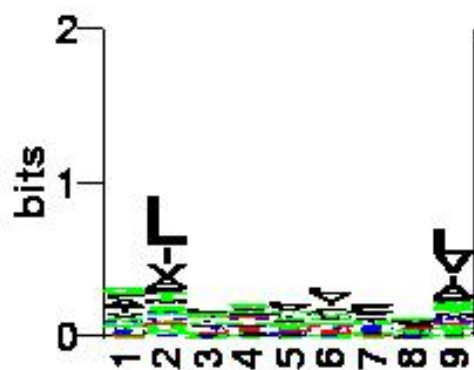
HLA-A1



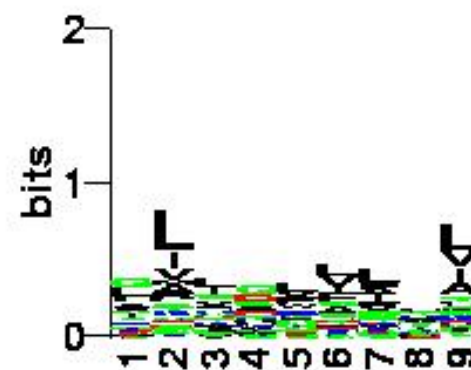
HLA-A*0201



HLA-A*0202



HLA-A*0203






COSMIC

Catalogue of somatic mutations in cancer

COSMIC

All cancers arise as a result of the acquisition of a series of fixed DNA sequence abnormalities, mutations, many of which ultimately confer a growth advantage upon... [\[More\]](#)

COSMIC Release v65

COSMIC v65 includes full curation of SH2B3, MAP2K1, MAP2K2, together with 5 new USP6 gene fusions, substantial updates are also made to growing TCGA and ICGC studies....[\[More\]](#) 

Statistics

Genes	24715	Unique Variants	873677
Samples	885051	Fusions	9014
Mutations	1146761	Genomic Rearrangements	7584
Papers	16514	Whole Genomes	6989

<http://cancer.sanger.ac.uk/cancergenome/projects/cosmic/>

Pancreatic Cancer

Cosmic » Tissue » Overview » Pancreas

Top genes

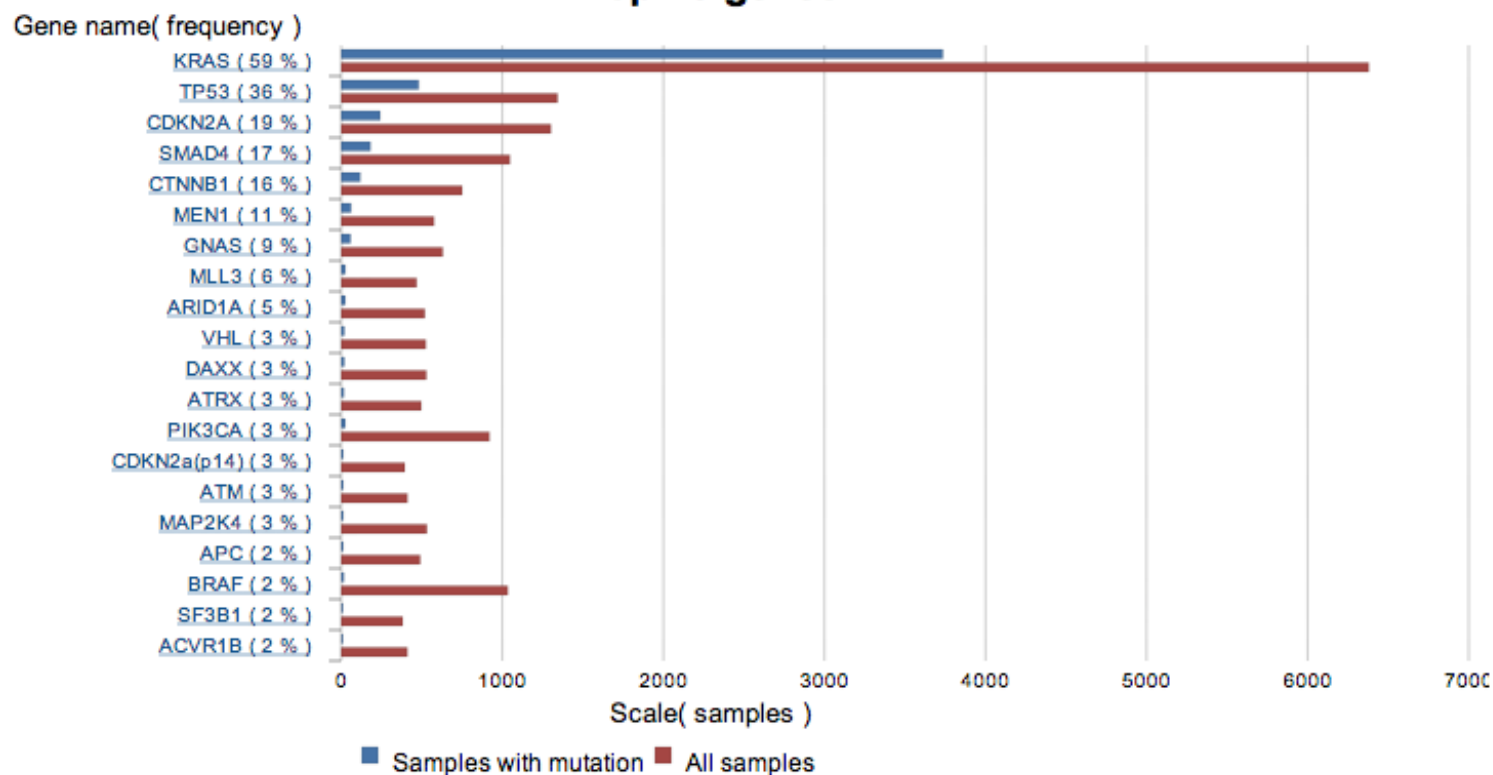
Fusion

Genes with Mutations

Genes without Mutations

Distribution

Top 20 genes



Malignant Melanoma

[Cosmic](#) » [Tissue](#) » [Overview](#) » [Skin](#)

Top genes

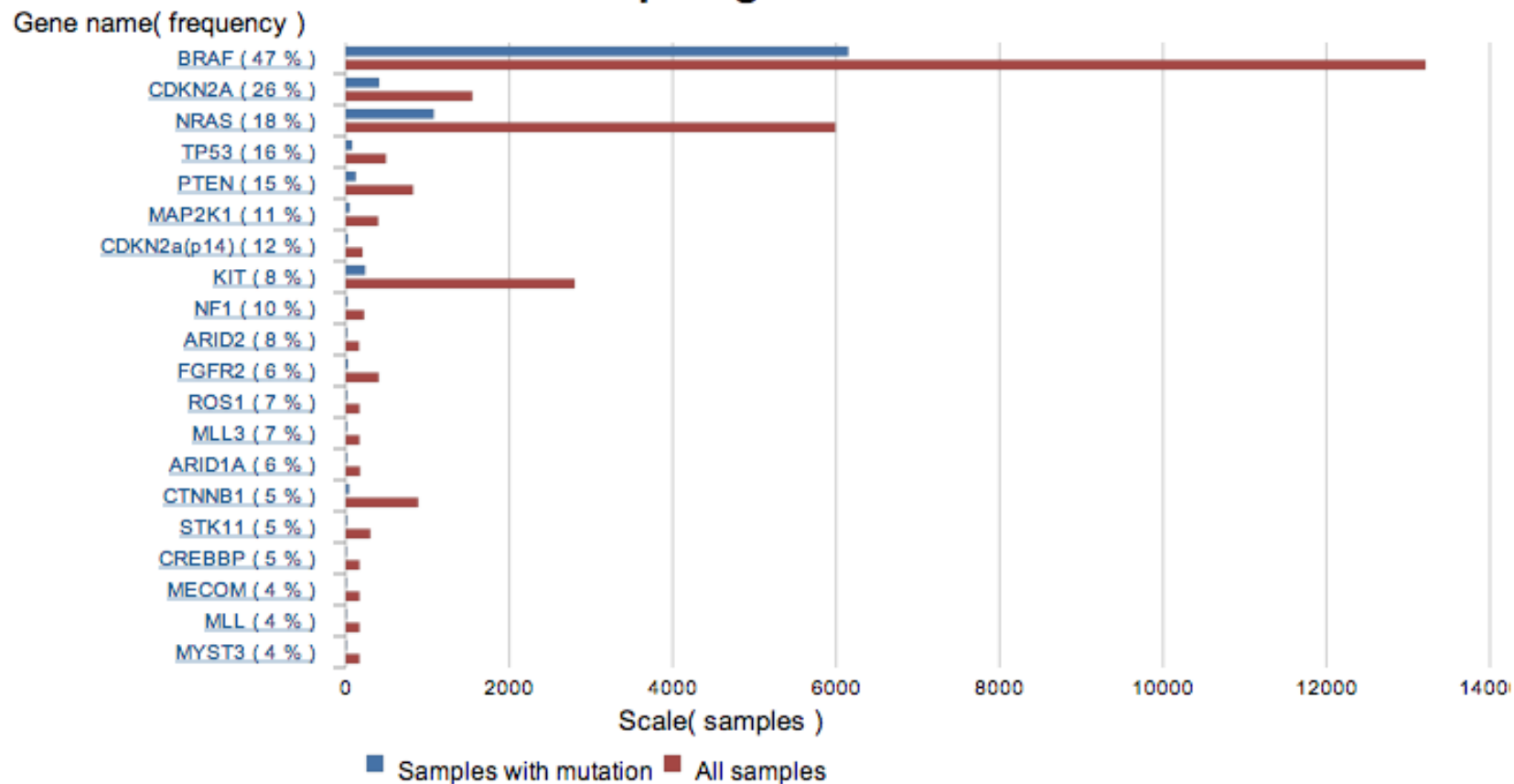
Fusion

Genes with Mutations

Genes without Mutations

Distribution

Top 20 genes



BRAF V600E

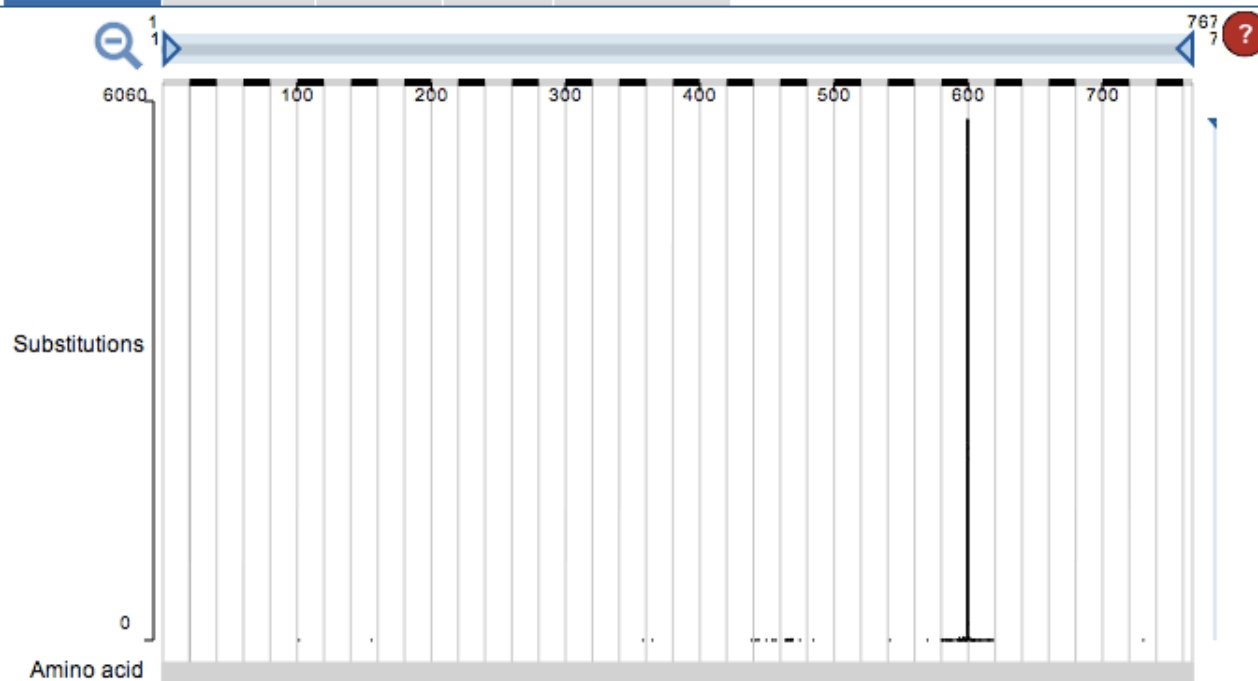


COSMIC

Catalogue of somatic mutations in cancer

Search [Home](#) [About](#) [Download](#) [Publications](#) [News](#) [Contact](#) [Help](#) [FAQ](#)

A A A A

[Cosmic](#) » [Gene](#) » [Analysis](#) » [BRAF](#)[Histogram](#) [Mutations](#) [Fusions](#) [Tissue](#) [Distribution](#)

Filters

Gene

Position

Start End

Sequence Type:

cDNA Amino Acid

Sites

 Skin

Histology

 Malignant Melanoma Systematic Screen Somatic Status Tumour Source Mutation Type 1000 Genomes Project



Children's Hospital
Informatics Program



Harvard
Medical School



RESEARCH PAPER

Oncolmunology 1:8, 1281–1289; November 2012; © 2012 Landes Bioscience

In silico prediction of tumor antigens derived from functional missense mutations of the cancer gene census

Jahan S. Khalili,^{1,†,*} Russell W. Hanson^{2,†} and Zoltan Szallasi^{2,3}

¹Departments of Melanoma Medical Oncology and Systems Biology; University of Texas M.D. Anderson Cancer Center; Houston, TX USA; ²Children's Hospital Informatics Program; Division of Health Sciences and Technology; Harvard–Massachusetts Institute of Technology; Harvard Medical School; Boston, MA USA; ³Department of Systems Biology; Center for Biological Sequence Analysis; Technical University of Denmark; Lyngby, Denmark

[†]These authors contributed equally to this work.

Keywords: cancer vaccines, computational biology, immunomics, immunotherapy, missense mutation, protein database, T cell therapy

Step	Action	Results
1	Mine COSMIC database	Known oncogenic mutations
2	Collect wildtype gene sequences and gene point mutations	250 genes 5,685 mutations
3	Generate peptide epitopes of 8, 9, 10, and 11-mers	76 strings/mutation 1,441,519 strings
4	Run NetMHC 3.2 binding affinity prediction artificial neural network algorithm	79 HLA alleles possible binding events = 31,566,629 epitopes scanned
5	Analyze complementary wildtype and mutated peptides for binding affinity	Develop and analyze facilitating and neutral mutations

How were the mutant and wildtype epitopes generated?

Examine an individual mutation:

KRAS position 12:

12p.G12?(50) p.G12A(1178) p.G12A(2) p.G12C(1) p.G12C(2478)
 p.G12C(3) p.G12D(7158)p.G12D(2) p.G12D(15) p.G12E(2)
 p.G12E(1) p.G12F(32) p.G12F(2) p.G12G(5) p.G12G(1)p.G12I(4)
 p.G12L(4) p.G12L(1) p.G12N(5) p.G12N(1) p.G12R(691) p.G12S(1118)
 p.G12S(1)p.G12V(3) p.G12V(4771) p.G12V(6) p.G12W(2) p.G12W(1) p.G12Y(2)

Generate epitopes of length 8, 9, 10, and 11 around the mutation site, with shifts to include all possible mutation-generated epitopes:

Shift Zero (0):

8mers

>G12V-wildtype-sequence-0-HLA-A0201 GGVGKSAL 22646
 >G12V-mutant-sequence-0-HLA-A0201 VGVGKSAL 22746

9mers

>G12V-wildtype-sequence-0-HLA-A0201 GGVGKSALT 23431
 >G12V-mutant-sequence-0-HLA-A0201 VGVGKSALT 23376

Shift One (1):

8mers

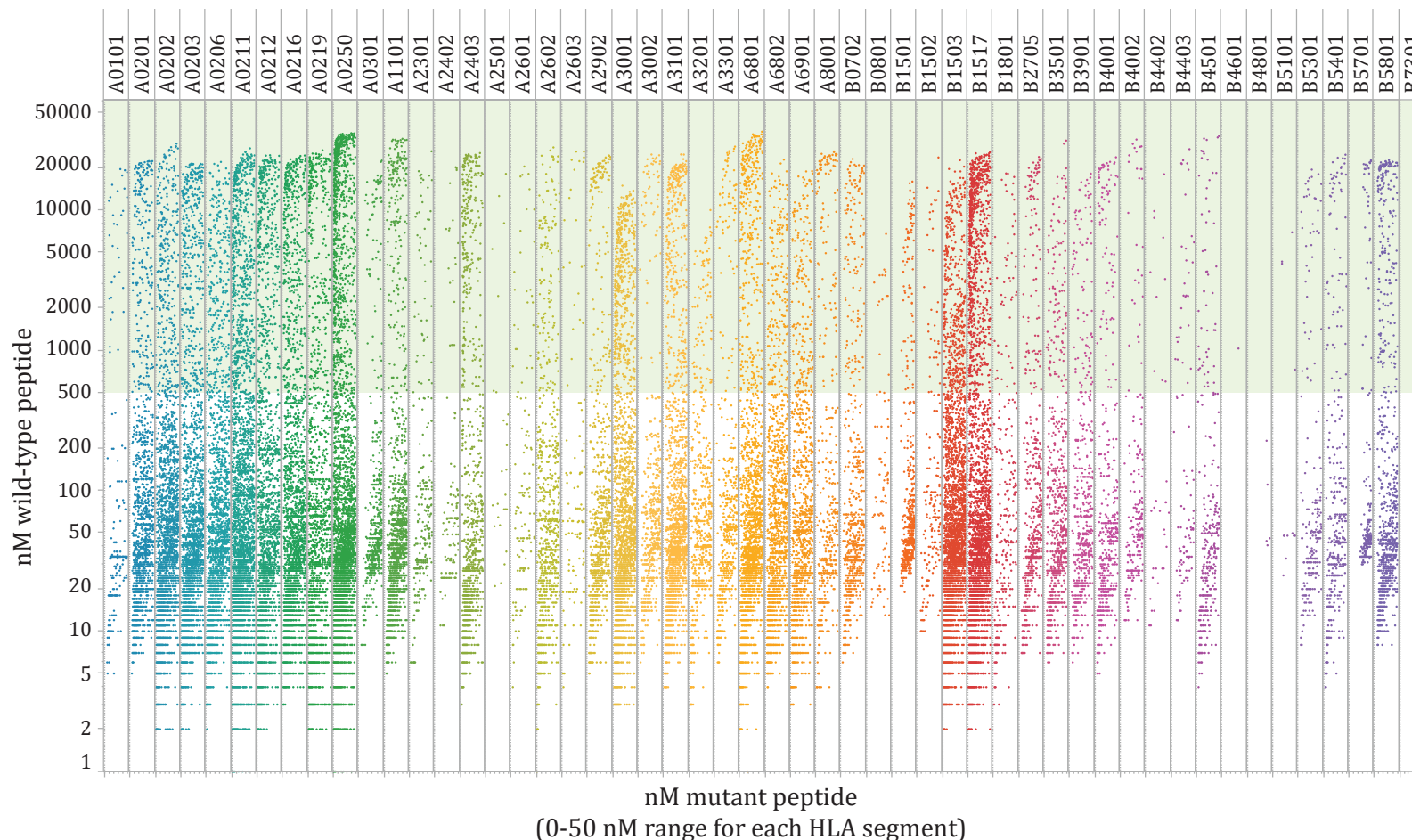
>G12V-wildtype-sequence-1-HLA-A0201 AGGVGKSA 24426
 >G12V-mutant-sequence-1-HLA-A0201 AVGVGKSA 19958

9mers

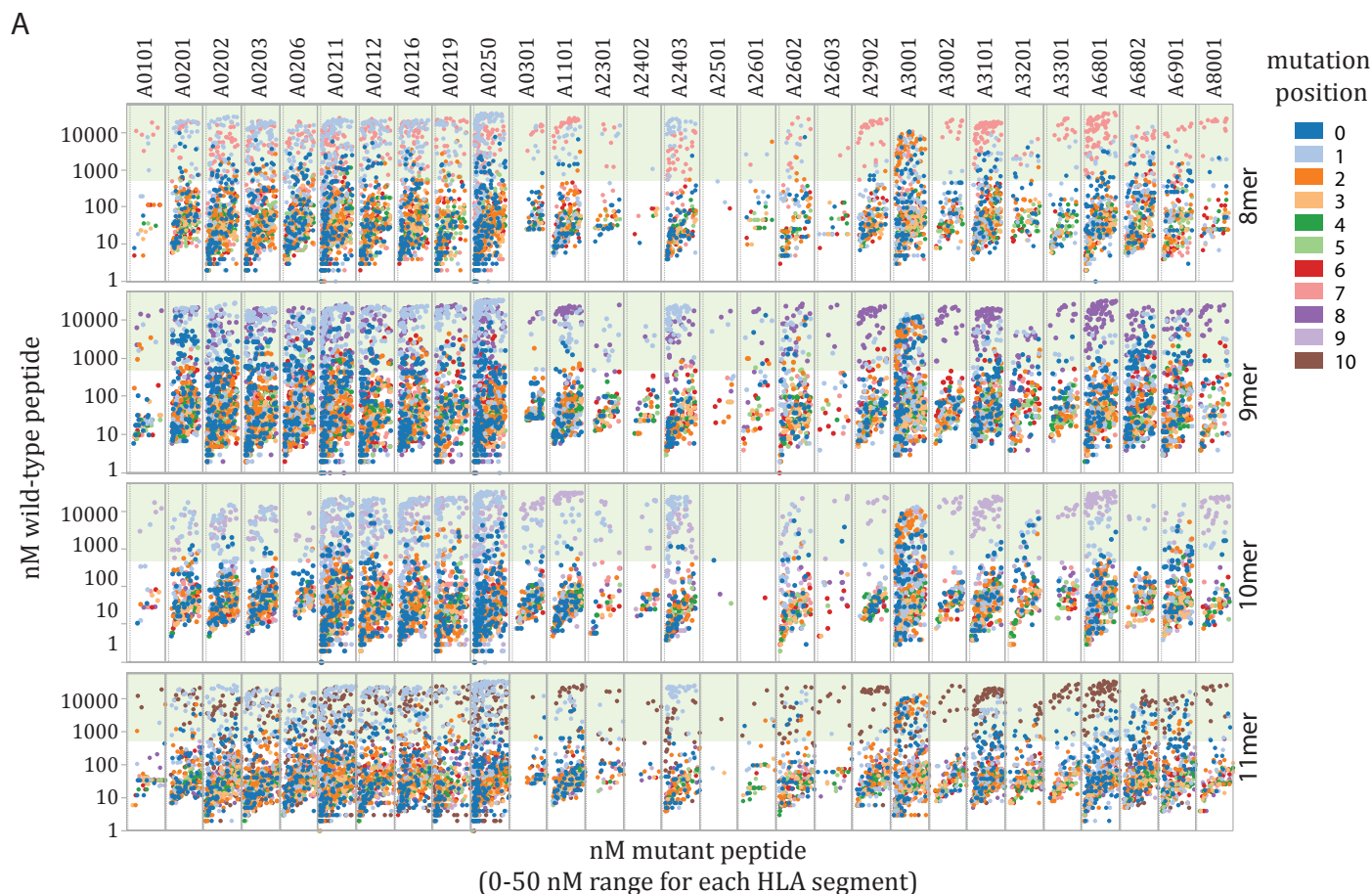
>G12V-wildtype-sequence-1-HLA-A0201 AGGVGKSAL 24412
 >G12V-mutant-sequence-1-HLA-A0201 AVGVGKSAL 19029

Wildtype Shift 0	GGVGKSALT
Wildtype Shift 1	AGGVGKSAL
Wildtype Shift 2	GAGGVGKSA
Wildtype Shift 3	VGAGGVGKS
Wildtype Shift 4	VVGAGGVGK
Wildtype Shift 5	VVVGAGGVG
Wildtype Shift 6	LVVVGAGGV
Wildtype Shift 7	KLVVVGAGG
Wildtype Shift 8	YKLVVVGAG
Mutant Shift 0	VGVGKSALT
Mutant Shift 1	AVGVGKSAL
Mutant Shift 2	GAVGVGKSA
Mutant Shift 3	VGAVGVGKS
Mutant Shift 4	VVGAVGVGK
Mutant Shift 5	VVVGAVGVG
Mutant Shift 6	LVVVGAVGV
Mutant Shift 7	KLVVVGAVG
Mutant Shift 8	YKLVVVGAV

--> Calculate MHC Class I binding affinity using NetMHC-3.2

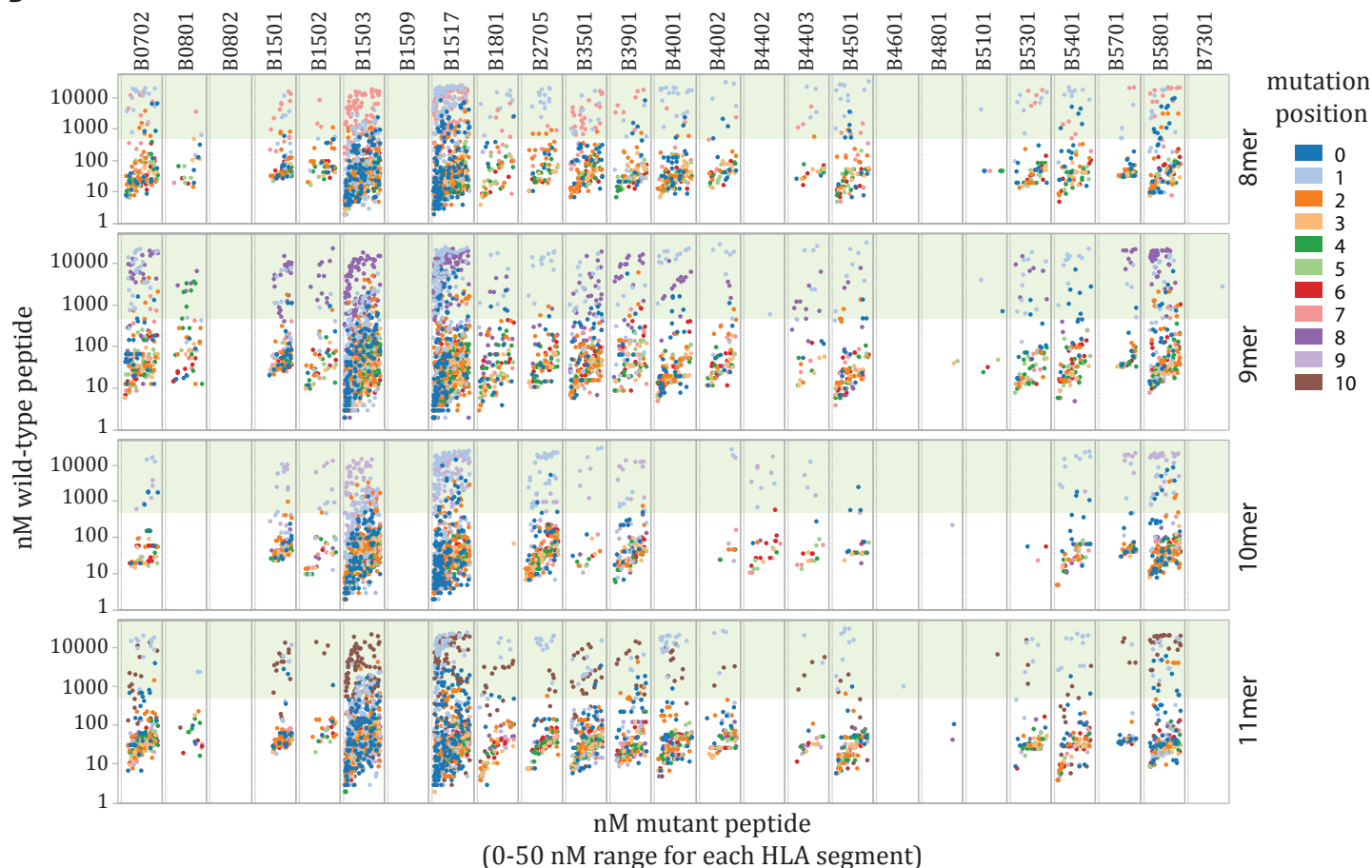


Facilitating mutation distribution for human HLA-A and HLA-B alleles. plot of tight binding mutated peptides (< 50 nM mutated peptide affinity score) from the cancer Gene census and corresponding wild-type peptides affinity score for each cognate hLa allele. Light green background indicates the threshold (500 nM) of predicted non-binding wild-type peptides.



Facilitating mutations utilize peripheral anchor residues. plot of tight binding mutated 8, 9, 10 and 11 mer peptides (mutated peptide affinity score < 50 nM) and corresponding wild-type peptides affinity score for each cognate hLa-a (a) and HLA-B (B) allele. Light green background indicates the threshold (500 nM) of predicted non-binding wild-type peptides. coloring indicates the position of each mutation in the peptide string (starting from the c terminus): dark blue (1), light blue (2), orange (3), light orange (4), dark green (5), light green (6), red (7), pink (8), purple (9), light purple (10), brown (11).

B



Facilitating mutations utilize peripheral anchor residues. plot of tight binding mutated 8, 9, 10 and 11 mer peptides (mutated peptide affinity score < 50 nM) and corresponding wild-type peptides affinity score for each cognate hLa-a (a) and HLA-B (B) allele. Light green background indicates the threshold (500 nM) of predicted non-binding wild-type peptides. coloring indicates the position of each mutation in the peptide string (starting from the c terminus): dark blue (1), light blue (2), orange (3), light orange (4), dark green (5), light green (6), red (7), pink (8), purple (9), light purple (10), brown (11).

Table 1. Facilitating, mutated strong binding HLA-A 02:01 peptides

FASTA wt	wt Peptide	nM (wt)	FASTA mt	mt Peptide	nM (mt)	Delta nM
>ALK-R401Q-wildtype-sequence-1-HLA-A0201	FRVALEYI	15009	>ALK-R401Q-mutant-sequence-1-HLA-A0201	FQVALEYI	29	14980
>BAP1-H169Q-wildtype-sequence-1-HLA-A0201	FHFVSYVPI	13143	>BAP1-H169Q-mutant-sequence-1-HLA-A0201	FQFVSYVPI	21	13122
>BRAF-K475M-wildtype-sequence-1-HLA-A0201	GKWHGDVAV	15489	>BRAF-K475M-mutant-sequence-1-HLA-A0201	GMWHGDVAV	13	15476
>CDK6-P199L-wildtype-sequence-1-HLA-A0201	TPVDLWSV	14601	>CDK6-P199L-mutant-sequence-1-HLA-A0201	TLVDLWSV	12	14589
>CHEK2-P536L-wildtype-sequence-1-HLA-A0201	RPAVCAAV	20392	>CHEK2-P536L-mutant-sequence-1-HLA-A0201	RLAVCAAV	25	20367
>EGFR-H773L-wildtype-sequence-8-HLA-A0201	VMASVDNPH	22464	>EGFR-H773L-mutant-sequence-8-HLA-A0201	VMASVDNPL	48	22416
>FANCF-P185L-wildtype-sequence-1-HLA-A0201	RPARFLSSL	22304	>FANCF-P185L-mutant-sequence-1-HLA-A0201	RLARFLSSL	38	22266
>GNAS-D141V-wildtype-sequence-8-HLA-A0201	SVMNVPDFD	20809	>GNAS-D141V-mutant-sequence-8-HLA-A0201	SVMNVPDFV	24	20785
>ITK-G372V-wildtype-sequence-7-HLA-A0201	FVQEIGSG	19247	>ITK-G372V-mutant-sequence-7-HLA-A0201	FVQEIGSV	48	19199
>JAK1-E966V-wildtype-sequence-8-HLA-A0201	FLPSGSLKE	17955	>JAK1-E966V-mutant-sequence-8-HLA-A0201	FLPSGSLKV	11	17944
>JAK2-K539L-wildtype-sequence-8-HLA-A0201	HMNQMVFKH	18253	>JAK2-K539L-mutant-sequence-8-HLA-A0201	HMNQMVFHL	35	18218
>KRAS-Q61L-wildtype-sequence-10-HLA-A0201	CLLDILDTAGQ	6354	>KRAS-Q61L-mutant-sequence-10-HLA-A0201	CLLDILDTAGL	26	6328
>NOTCH1-R1634L-wildtype-sequence-1-HLA-A0201	KRAAEGWAA	21734	>NOTCH1-R1634L-mutant-sequence-1-HLA-A0201	KLAAEGWAA	24	21710
>RB1-P515L-wildtype-sequence-1-HLA-A0201	FPWILNVL	10736	>RB1-P515L-mutant-sequence-1-HLA-A0201	FLWILNVL	13	10723
>TP53-P47L-wildtype-sequence-8-HLA-A0201	AMDDLMLSP	10776	>TP53-P47L-mutant-sequence-8-HLA-A0201	AMDDLMLSL	11	10765



Children's Hospital
Informatics Program



Harvard
Medical School



So, what has this database accomplished?

An experimentalist can test MHC binding for 10-20 epitopes in a month

We tested 32,000,000, and got a database of 65,000 leads.

$32,000,000 \text{ total} / 20 \text{ epitopes} = 1,600,000$

$1,600,000 / 12 \text{ months} = 133,333 \text{ years}$

We are currently doing a follow-up collaboration with a wetlab immunologist to test epitope binding in HLA types prevalent in Denmark



Children's Hospital
Informatics Program



Harvard
Medical School



Expert Opin Biol Ther. 2007 Apr;7(4):543-54.

PANVAC-VF: poxviral-based vaccine therapy targeting CEA and MUC1 in carcinoma.

Madan RA, Arlen PM, Gulley JL.

Clinical Immunotherapy Group, National Cancer Institute (NCI), Laboratory of Tumor Immunology and Biology, National Institutes of Health (NIH), 10 Center Drive, Bethesda, MD 20892, USA.

PANVAC is a cancer vaccine therapy delivered through two viral vectors--recombinant vaccinia and recombinant fowlpox--which are given sequentially. Both vectors contain transgenes for the tumor-associated antigens epithelial mucin 1 and carcinoembryonic antigen, which are altered or overexpressed in most carcinomas. The vectors also contain transgenes for three human T cell costimulatory molecules required to enhance immune response: B7.1, intracellular adhesion molecule-1 and leukocyte function-associated antigen-3. PANVAC is injected subcutaneously and processed by the body's antigen-presenting cells. Preclinical studies have demonstrated the efficacy of PANVAC in inducing both carcinoembryonic antigen- and mucin 1-specific cytotoxic T lymphocyte responses in vitro and in murine models. Other strategies that enhance the immune response include the use of granulocyte-macrophage colony-stimulating factor and a prime-boost administration sequence. Clinical trials have demonstrated PANVAC's safety and its ability to induce antigen-specific T cell responses. Early clinical trials are evaluating PANVAC alone and in combination with conventional chemotherapy and/or radiation. Studies to date hold promise for the use of PANVAC as a means to stimulate the immune system against malignancies and to provide clinical benefit.

<http://clinicaltrials.gov/show/NCT00088660>



Children's Hospital
Informatics Program



Harvard
Medical School



PROVAC – Prostate cancer vaccine

Scientists at AV Therapeutics believe that there are two problems which need to be solved. The first is that *cancer antigens, in part, are self-aberrant proteins that evade the immune system and hence are unrecognized and not killed by the host's immune system.* The host's immune system needs to be re-educated so that cancer cells can be recognized and killed. The second problem is the constant generation of random mutations in cellular proteins and the generation of a large number of ever changing antigenic epitopes. The Company's proprietary vaccine technology overcomes both of these limitations by using therapeutic peptides that are mimics of the multivalent antigens.

The objective of the first clinical testing of these peptides (ProVac-1,3,5) would be to render prostate cancer patients vaccinated with these peptides cancer-free. These are patients who have undergone the present standard of care for prostate cancer and these peptides are being tested for secondary prevention of prostate cancer recurrences. The next logical step for the clinical development of these peptide cancer vaccines would be the primary prevention of prostate cancer. Using our pipeline of patented products, our near term objective is to combine Capridine, the newly discovered and AVT-patented proprietary prostate-cancer-targeted chemotherapeutic drug, with a peptide-based immunotherapeutic vaccine, to design a completely unique curative treatment regimen for prostate cancer.



Children's Hospital
Informatics Program



Harvard
Medical School



Human Molecular Genetics, 2012, Vol. 21, Review Issue 1 R29–R36
doi:10.1093/hmg/dds384
Advance Access published on September 12, 2012

Interrogating the major histocompatibility complex with high-throughput genomics

Paul I.W. de Bakker^{1,2,3,5,*} and Soumya Raychaudhuri^{3,4,5,6,7}

¹Department of Medical Genetics, and ²Department of Epidemiology, University Medical Center Utrecht, Utrecht, The Netherlands, ³Division of Genetics, and ⁴Division of Rheumatology, Brigham and Women's Hospital, Harvard Medical School, Boston, MA, USA, ⁵Program in Medical and Population Genetics, Broad Institute of Harvard and MIT, Cambridge, MA, USA, ⁶Partners HealthCare Center for Personalized Genetic Medicine, Boston, MA, USA, and ⁷Faculty of Medical and Human Sciences, University of Manchester, Manchester, UK

Received August 19, 2012; Revised and Accepted September 6, 2012

The major histocompatibility complex (MHC) region on the short arm of chromosome 6 harbors the largest number of replicated associations across the human genome for a wide range of diseases, but the functional basis for these associations is still poorly understood. One fundamental challenge in fine-mapping associations to functional alleles is the enormous sequence diversity and broad linkage disequilibrium of the MHC, both of which hamper the cost-effective interrogation in large patient samples and the identification of causal variants. In this review, we argue that there is now a valuable opportunity to leverage existing genome-wide association study (GWAS) datasets for in-depth investigation to identify independent effects in the MHC. Application of imputation to GWAS data facilitates comprehensive interrogation of the classical human leukocyte antigen (HLA) loci. These datasets are, in many cases, sufficiently large to give investigators the ability to disentangle effects at different loci. We also explain how querying variation at individual amino acid positions for association can be powerful and expand traditional analyses that focus only on the classical HLA types.

Training set: Type 1 Diabetes Genetics Consortium

ORIGINAL ARTICLE

HLA DR-DQ Haplotypes and Genotypes and Type 1 Diabetes Risk

Analysis of the Type 1 Diabetes Genetics Consortium Families

Henry Erlich,^{1,2} Ana Maria Valdes,² Janelle Noble,² Joyce A. Carlson,³ Mike Varney,⁴ Pat Concannon,⁵ Josyf C. Mychaleckyj,⁵ John A. Todd,⁶ Persia Bonella,² Anna Lisa Fear,² Eva Lavant,³ Anthony Louey,⁴ and Priscilla Moonsamy¹ for the Type 1 Diabetes Genetics Consortium

OBJECTIVE—The Type 1 Diabetes Genetics Consortium has collected type 1 diabetic families worldwide for genetic analysis. The major genetic determinants of type 1 diabetes are alleles at the HLA-DRB1 and DQB1 loci, with both susceptible and protective DR-DQ haplotypes present in all human populations. The aim of this study is to estimate the risk conferred by specific DR-DQ haplotypes and genotypes.

RESEARCH DESIGN AND METHODS:—Six hundred and

DQA1, and DQB1 loci determine the extent of haplotypic risk. The comparison of closely related DR-DQ haplotype pairs with different type 1 diabetes risks allowed identification of specific amino acid positions critical in determining disease susceptibility. These data also indicate that the risk associated with specific HLA haplotypes can be influenced by the genotype context and that the *trans*-complementing heterodimer encoded by DQA1*0501 and DQB1*0302 confers very high risk. *Diabetes* 57: 1084–1092, 2008

This method allowed us to do HLA typing of over 45,000 patient case and control SNP arrays

CasePresent	CaseAbsent	ControlPresent	ControlAbsent	OddsRatioControl	OddsRatioCase	chi square control	chi square case	OddsRatio2	OR 95% CI -	OR 95% CI+	SE	p-value
92	2540	115	6878	0.461616749	2.166299213	31.13188175	31.13188175	2.166299213	1.640682317	2.860302297	0.141789666	2.41079E-08
115	2496	170	6776	0.544530568	1.836444193	25.12017138	25.12017138	1.836444193	1.443070385	2.337047833	0.122988722	5.38664E-07
375	2024	1237	4868	1.37150808	0.729124396	24.03793913	24.03793913	0.729124396	0.642397512	0.827560195	0.0646109	9.44561E-07
111	2500	168	6774	0.558574518	1.790271429	22.44027341	22.44027341	1.790271429	1.402530419	2.285204823	0.124535189	2.1678E-06
387	2016	1251	4856	1.342017547	0.74514674	21.28270785	21.28270785	0.74514674	0.657408349	0.84459512	0.06391637	3.9629E-06
113	2496	177	6754	0.578866408	1.727514305	20.31689966	20.31689966	1.727514305	1.358321534	2.197052322	0.122670194	6.56184E-06
325	2096	1066	5114	1.344325381	0.743867529	18.77282069	18.77282069	0.743867529	0.650453023	0.850698055	0.068466417	1.47251E-05
374	2018	1197	4898	1.318636003	0.758359394	18.2540235	18.2540235	0.758359394	0.667807721	0.861189779	0.064876219	1.93317E-05



Children's Hospital
Informatics Program



Harvard
Medical School



Using computation and imputation
to drive experiments and further
directed sequencing of specific regions
-- Sandor awesome wet lab guy does experiments!!
(Sandor doesn't use the internet much so I couldn't find a
nice picture of him ☹)



Children's Hospital
Informatics Program



Harvard
Medical School



TISSUE ANTIGENS
IMMUNE RESPONSE GENETICS



Multi-locus HLA class I and II allele and haplotype associations with follicular lymphoma

C. F. Skibola¹, N. K. Akers¹, L. Conde¹, M. Ladner², S. K. Hawbecker², F. Cohen², F. Ribas², H. A. Erlich^{2,3}, D. Goodridge⁴, E. A. Trachtenberg², M. T. Smith¹ & P. M. Bracci⁵

1 Division of Environmental Health Sciences, School of Public Health, University of California, Berkeley, CA, USA

2 Center for Genetics, Children's Hospital Oakland Research Institute, Oakland, CA, USA

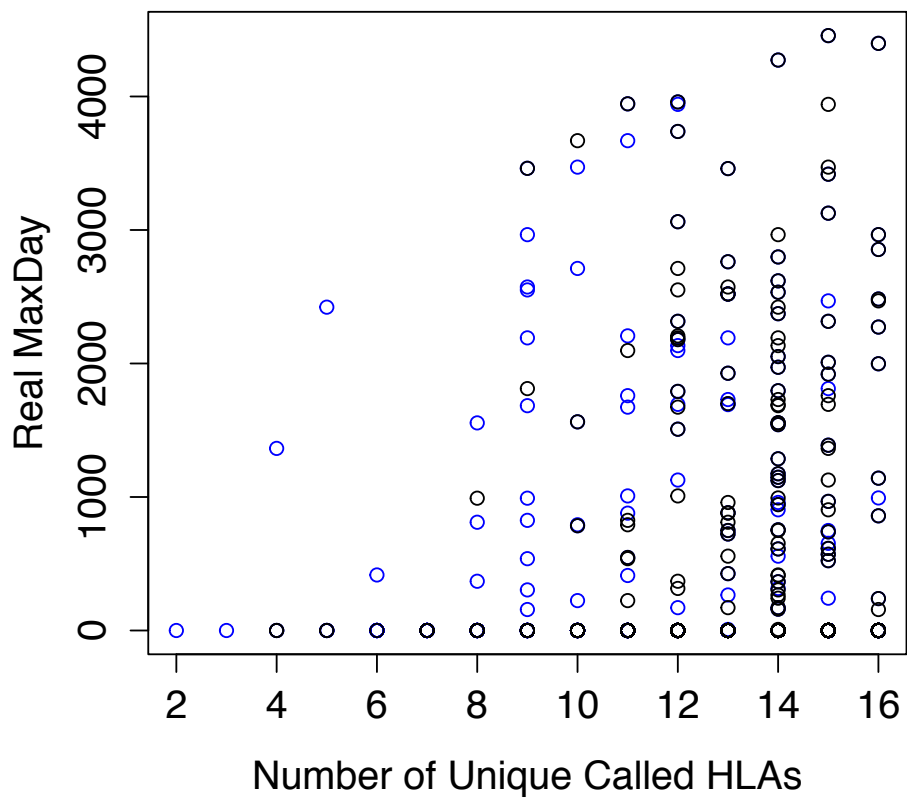
3 Conexio Genomics, Perth, Australia

4 Roche Molecular Systems, Alameda, CA, USA

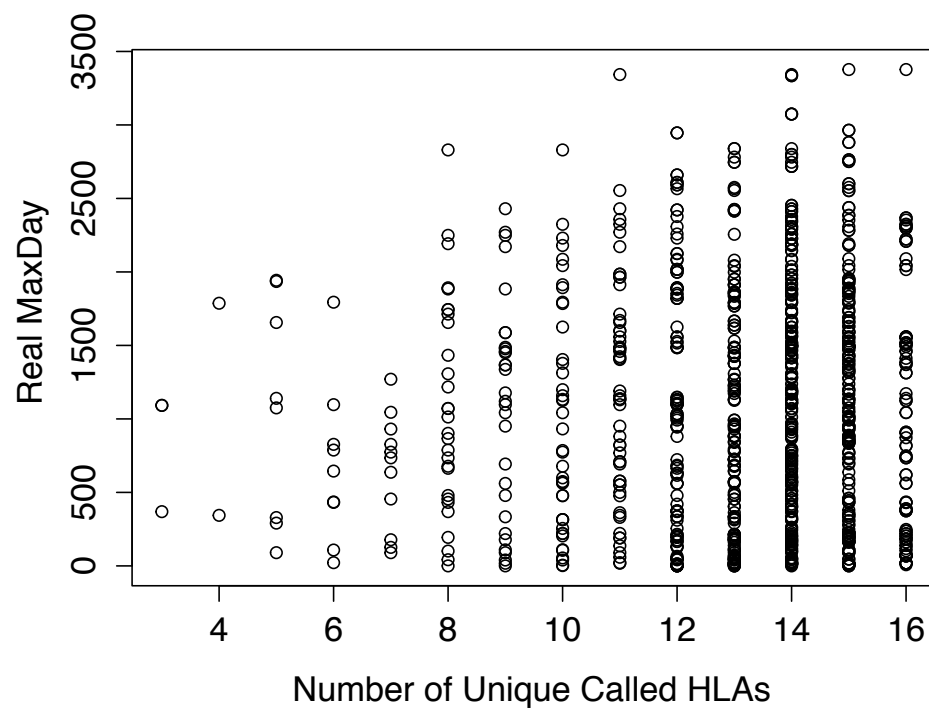
5 Department of Epidemiology and Biostatistics, School of Medicine, University of California San Francisco, San Francisco, CA, USA

Located in the HLA class I region at 6p21.33 near psoriasis susceptibility region 1, rs6457327 was inversely associated with risk of FL (P-value = 4.7×10^{-11}) (8). In the HLA class II region at 6p21.32, two single nucleotide polymorphisms (SNPs), rs10484561 and rs7755224, were associated with twofold increased risks of FL (P-values = 1.12×10^{-29} and 2.0×10^{-19} , respectively) (7). rs10484561 and rs7755224 are in total linkage disequilibrium (LD) and are located 29 and 16 kb centromeric of HLA-DQB1, respectively. On the basis of a tag SNP analysis, we inferred that rs10484561 may be part of a high-risk extended haplotype, DRB1*01:01-DQA1*01:01-DQB1*05:01 (7). Another class II locus in the HLA-DQB1 region, rs2647012, was inversely associated with FL risk after adjusting for rs10484561 [Odds ratio (OR) = 0.70, P-value = 4×10^{-12}] (9).

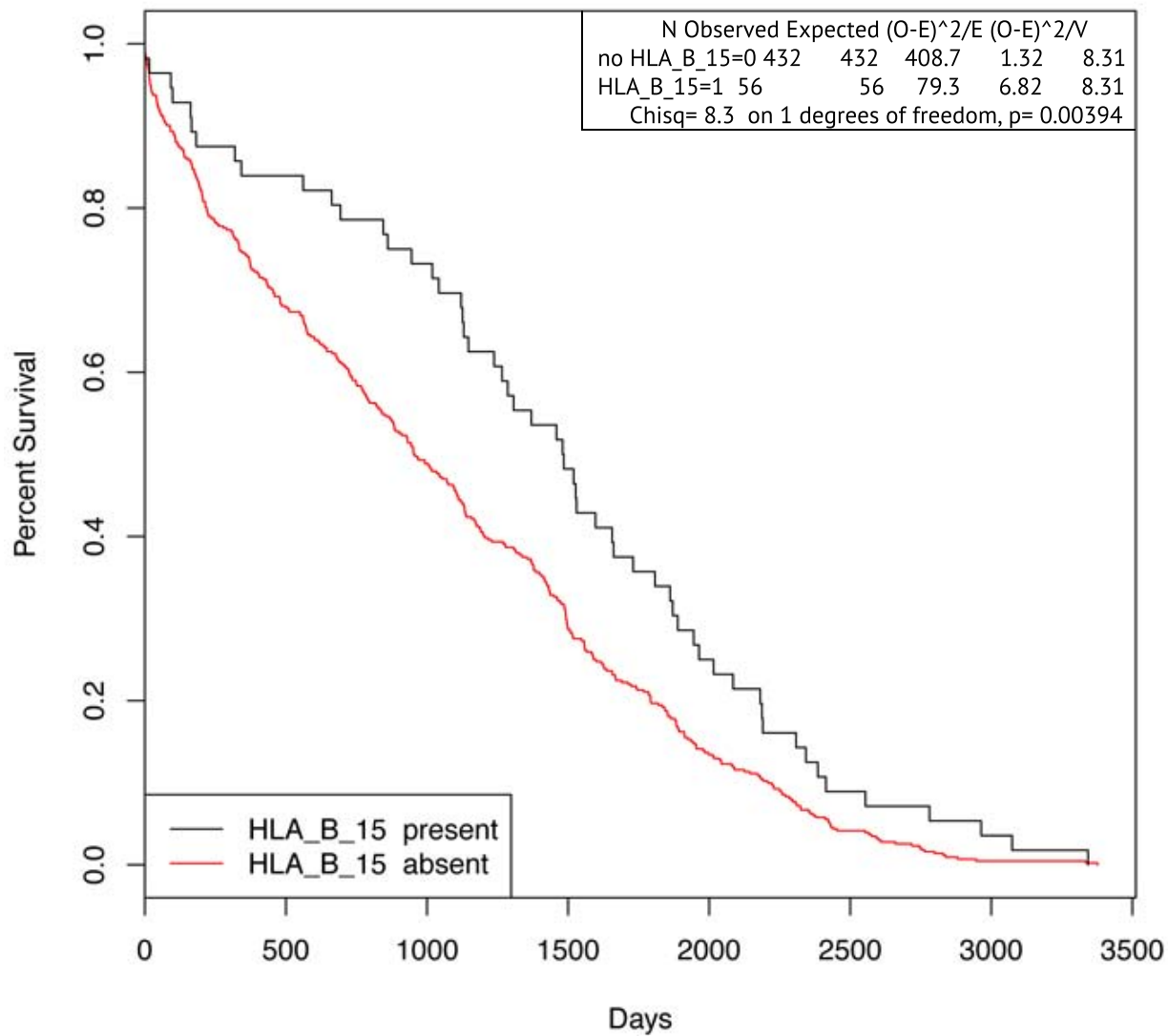
Breast TCGA Survival vs. Complexity of HLAs (n=821, blue=tumor)



Renal TCGA Survival vs. Complexity of HLAs (n=1042)



TCGA Renal Survival Plot



Food for thought: How to use the contrapositive to prove/disprove drug/food safety

$$(A \rightarrow B) \rightarrow (\neg B \rightarrow \neg A)$$

For example, if we want to prove that every girl in the United States (A) is blonde (B), we can either try to directly prove $(A \rightarrow B)$ by checking all girls in the United States to see if they are all blonde. Alternatively, we can try to prove $(\neg B \rightarrow \neg A)$ by checking all non-blonde girls to see if they are all outside the US. This means that if we find at least one non-blonde girl within the US, we will have disproved $(\neg B \rightarrow \neg A)$, and equivalently $(A \rightarrow B)$.

To conclude, for any statement where A implies B , then not B always implies not A . Proving or disproving either one of these statements automatically proves or disproves the other. They are fully equivalent.



AQ: A

From the Dana-Farber Cancer Institute; Brigham and Women's Hospital; Children's Hospital Informatics Program at the Harvard-MIT Division of Health Sciences and Technology; Massachusetts General Hospital Cancer Center; and Beth Israel Deaconess Hospital, Harvard Medical School; Harvard School of Public Health, Boston, MA; Center for Biological Sequence Analysis, BioCentrum-Technical University of Denmark, Lyngby, Denmark; Cancer Institute of New Jersey, Robert Wood Johnson Medical School, University of Medicine and Dentistry of New Jersey, New Brunswick, NJ.

AQ: B

Submitted February 13, 2009; accepted October 23, 2009; published online ahead of print at www.jco.org on Month XX, 2009.

Supported by Grants No. CA089393 from the National Cancer Institute Program of Research Excellence (SPORE) in Breast Cancer at the Dana-Farber/Harvard Cancer Center and No. R21LM008823-01A1 from the National Institutes of Health, and by the Breast Cancer Research Foundation, Sidney

Efficacy of Neoadjuvant Cisplatin in Triple-Negative Breast Cancer

Daniel P. Silver, Andrea L. Richardson, Aron C. Eklund, Zhigang C. Wang, Zoltan Szallasi, Qiyuan Li, Nicolai Juul, Chee-Onn Leong, Diana Calogrias, Ayodele Buraimoh, Aquila Fatima, Rebecca S. Gelman, Paula D. Ryan, Nadine M. Tung, Arcangela De Nicolo, Shridar Ganesan, Alexander Miron, Christian Colin, Dennis C. Sgroi, Leif W. Ellisen, Eric P. Winer, and Judy E. Garber

A B S T R A C T

Purpose

Cisplatin is a chemotherapeutic agent not used routinely for breast cancer treatment. As a DNA cross-linking agent, cisplatin may be effective treatment for hereditary **BRCA1**-mutated breast cancers. Because sporadic triple-negative breast cancer (TNBC) and **BRCA1**-associated breast cancer share features suggesting common pathogenesis, we conducted a neoadjuvant trial of cisplatin in TNBC and explored specific biomarkers to identify predictors of response.

Patients and Methods

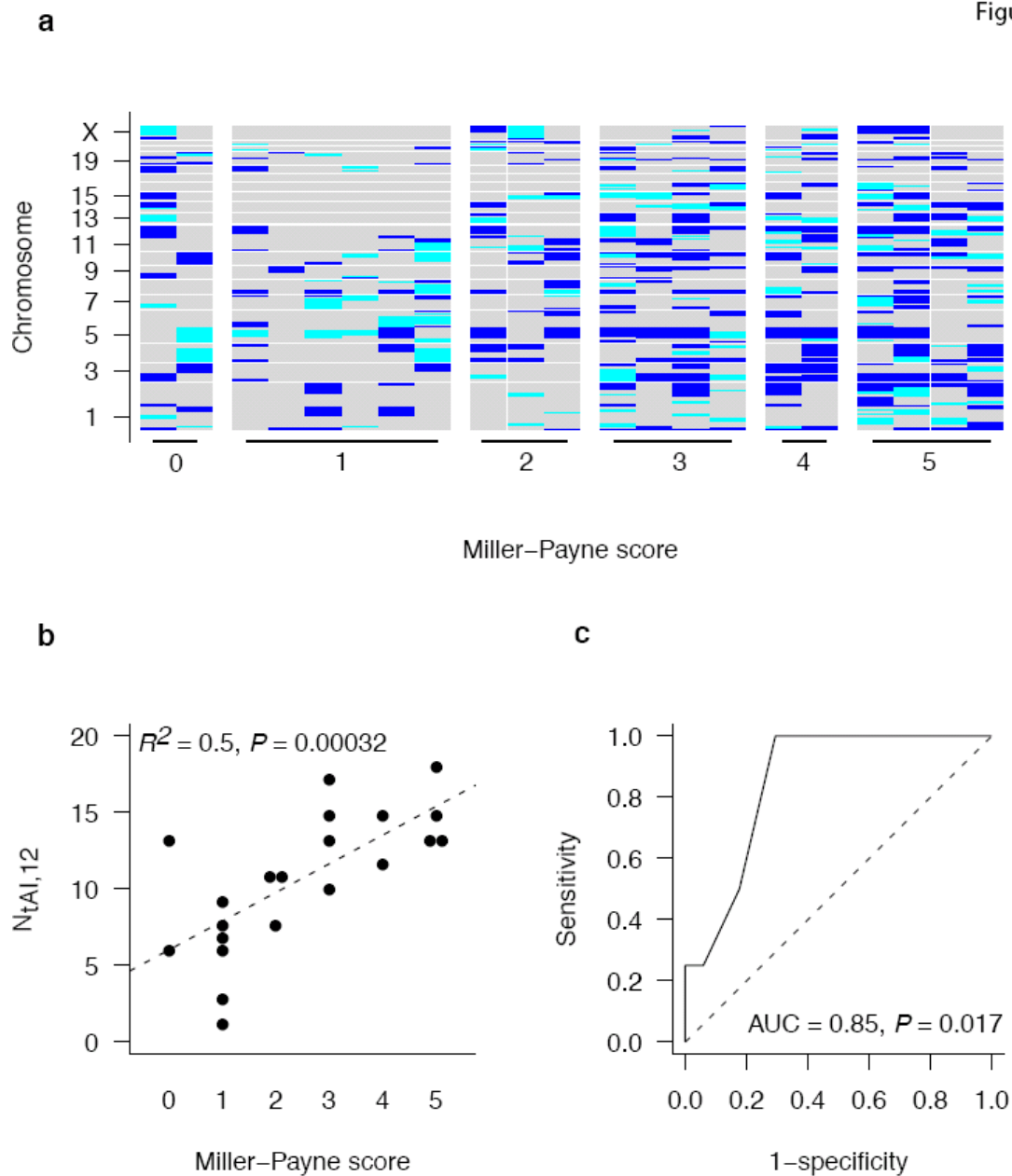
Twenty-eight women with stage II or III breast cancers lacking estrogen and progesterone receptors and HER2/Neu (TNBC) were enrolled and treated with four cycles of cisplatin at 75 **AQ:C-D** mg/m² every 21 days. After definitive surgery, patients received standard adjuvant chemotherapy and radiation therapy per their treating physicians. Clinical and pathologic treatment response were assessed, and pretreatment tumor samples were evaluated for selected biomarkers.

Results

Six (22%) of 28 patients achieved pathologic complete responses, including both patients with **BRCA1** germline mutations; 18 (64%) patients had a clinical complete or partial response. Fourteen

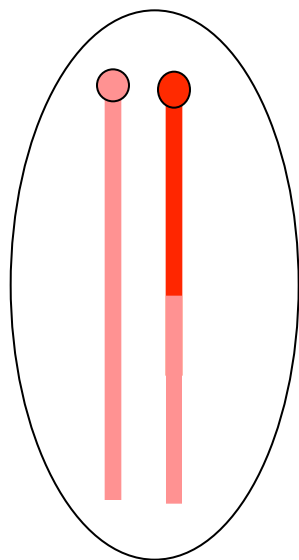
Correlation with tAI in cisplatin treated TNBC cohort

Figure 2



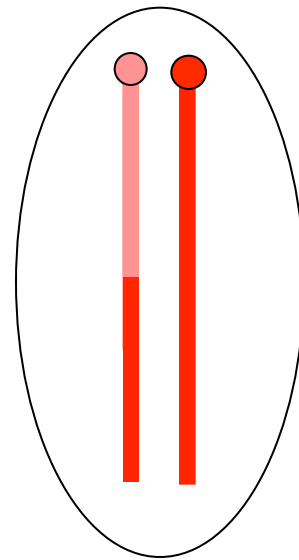
After mitosis

- **Telomeric loss**
- **Duplication**
- **LOH with normal copy number**



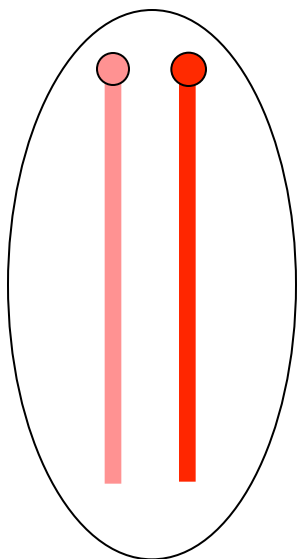
+

- **Telomeric loss**
- **Duplication**
- **LOH with normal copy number**



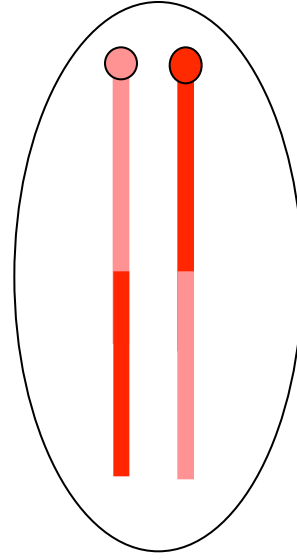
OR

- **No LOH**
- **Normal 2 copies**

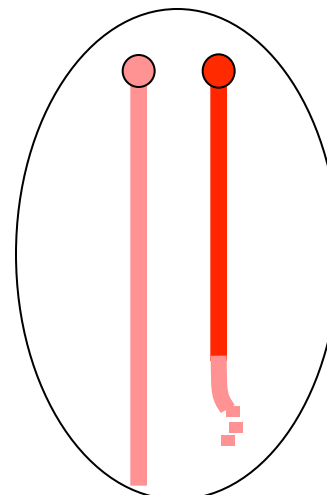
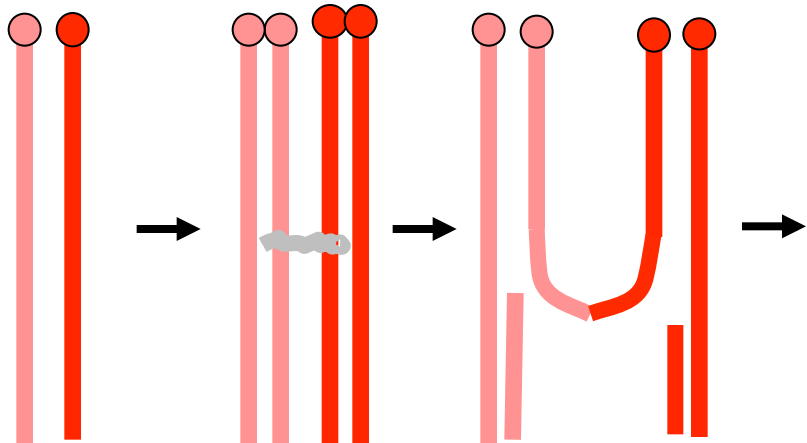


+

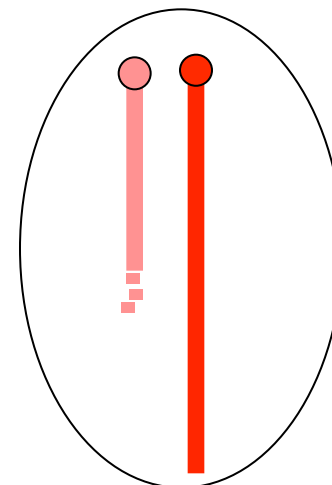
- **No LOH**
- **Normal 2 copies**



Formation of Quadriradials II

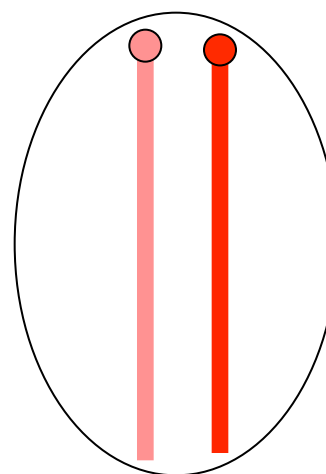


**LOH with
partial deletion**

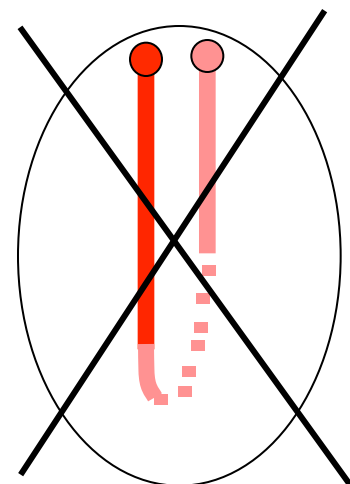


**LOH with
deletion**

OR

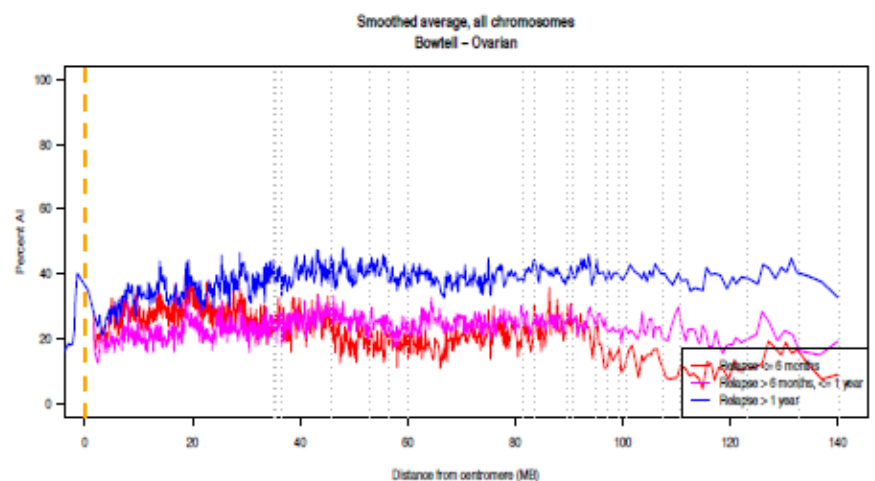
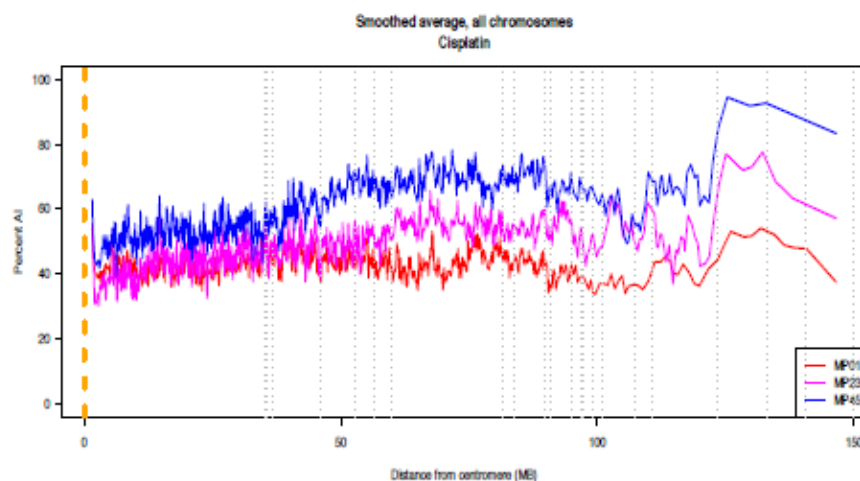
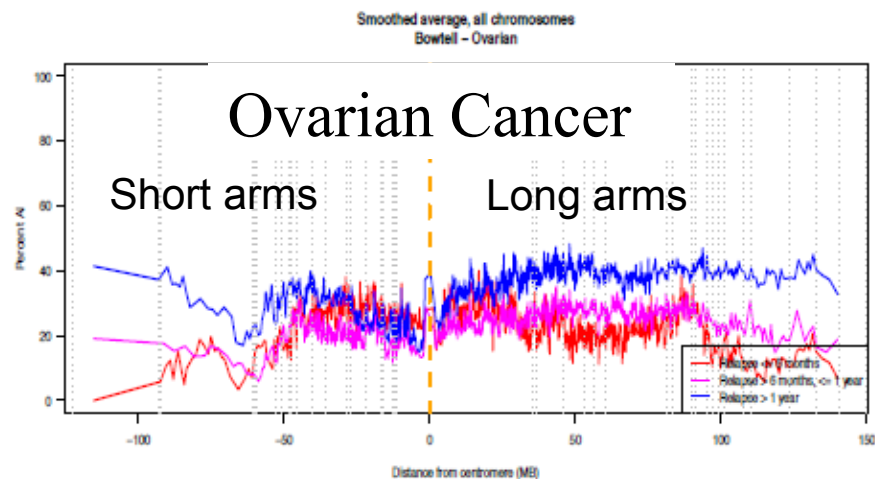
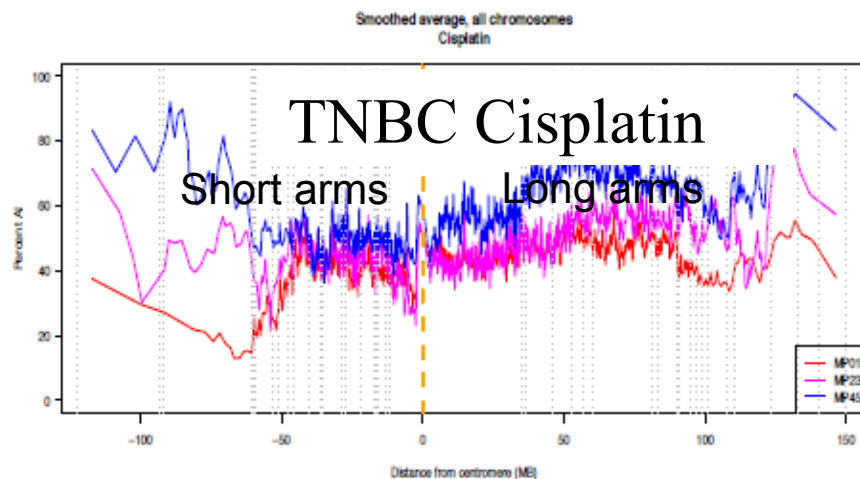


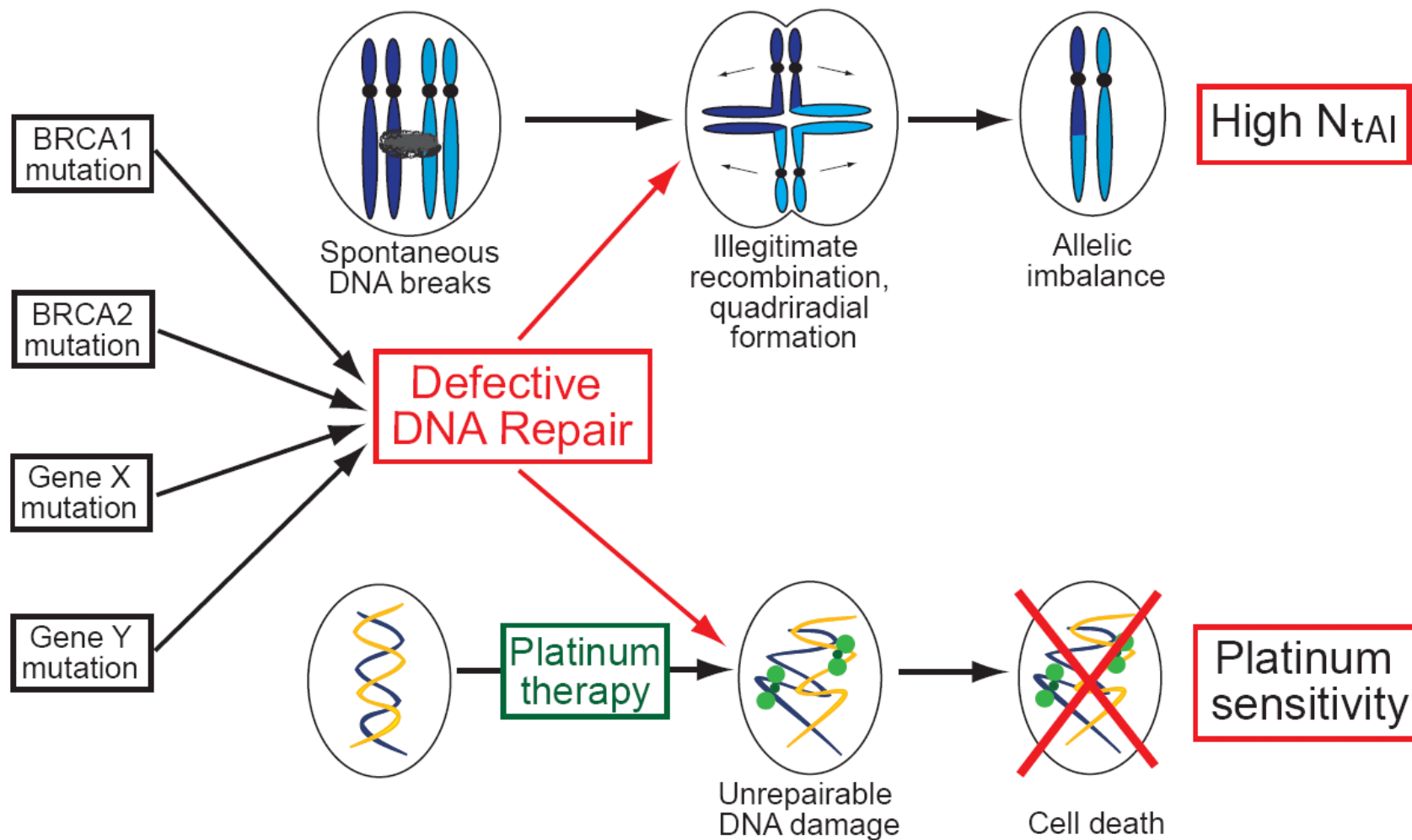
Normal



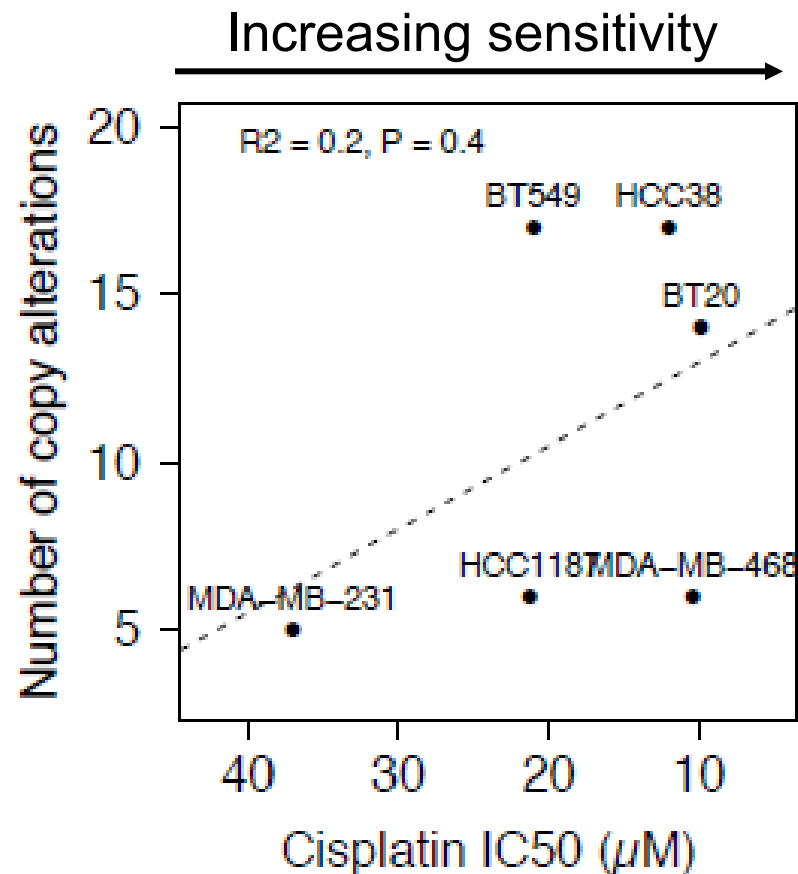
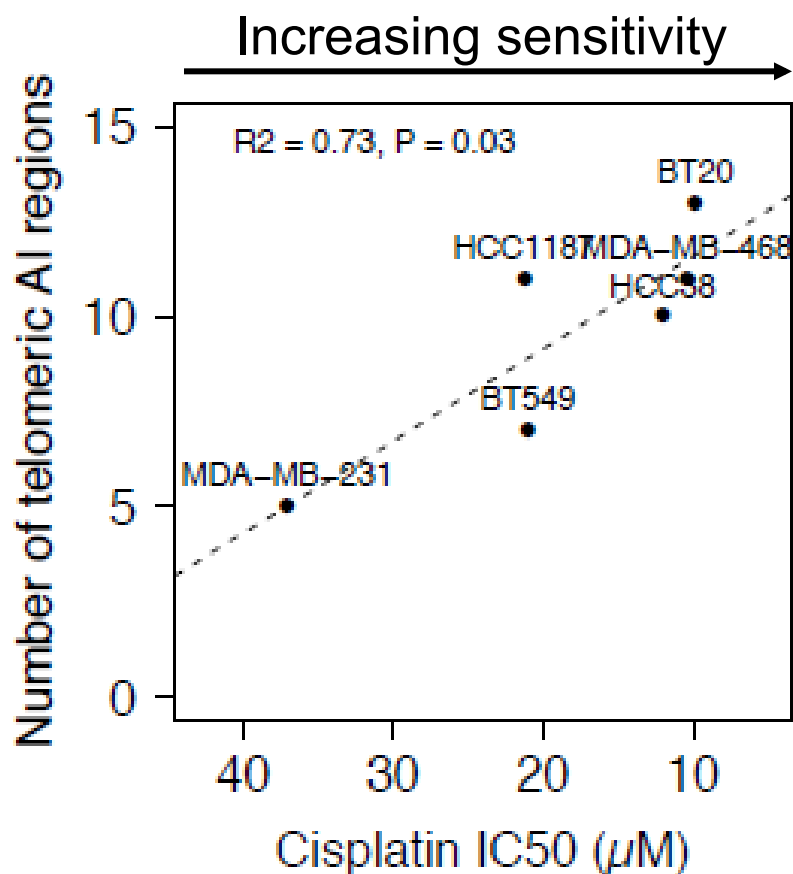
**Dead or soon
to be dead**

We analyzed the frequency of AI for each SNP as a function of distance from centromere:
high frequency of telomeric loss



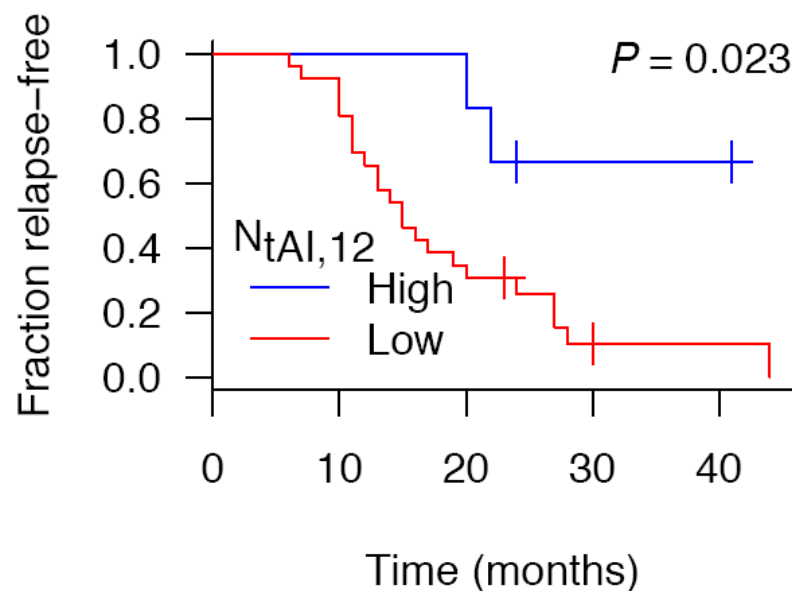
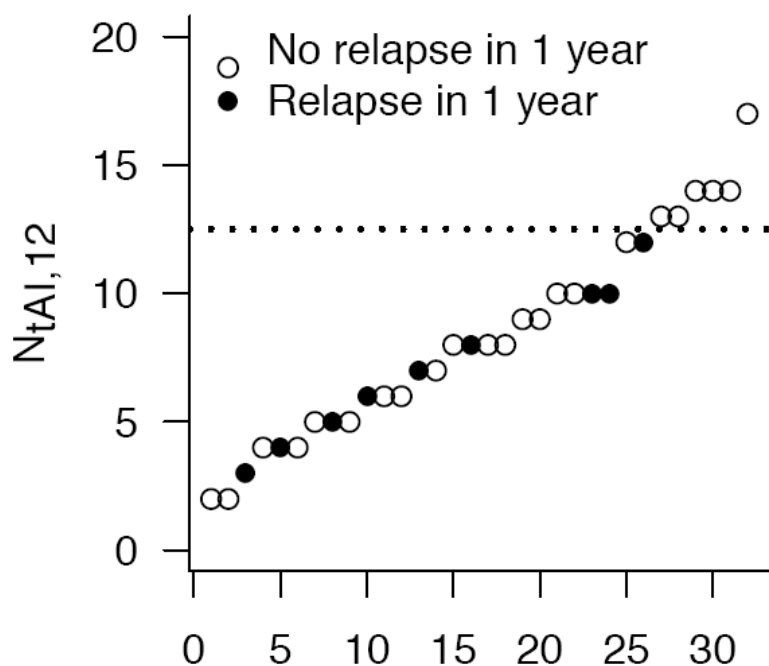


The number of regions of telomeric AI (≥ 19 Mb) was highly correlated with cisplatin sensitivity in TNBC cell lines.

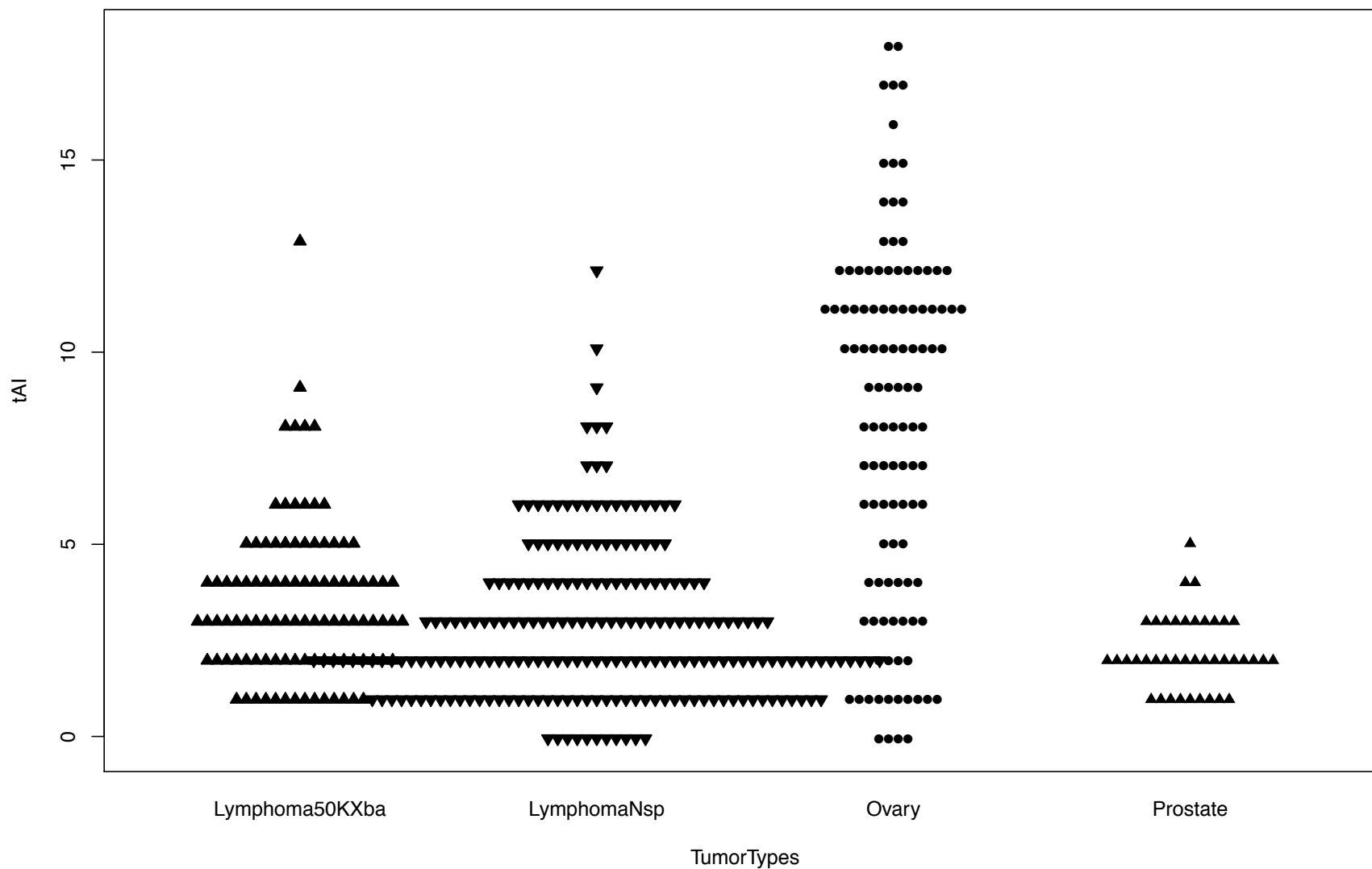


We next evaluated a public SNP array dataset of primary ovarian cancers treated with cisplatin (plus Taxol) with clinical outcome data

K-M using $N_{tAI, 19} \geq 10$ based on best sensitivity for pCR in TNBC trial



number at risk				
6	6	6	2	2
27	24	9	2	1



Single nucleotide polymorphisms and risk of recurrence of renal-cell carcinoma: a cohort study

Findings We included 554 patients (403 in the discovery cohort and 151 in the validation cohort). We successfully genotyped 290 single nucleotide polymorphisms in the discovery cohort, but excluded five because they did not have a variant group for comparison. The polymorphism rs11762213, which causes a synonymous aminoacid change in *MET* (144G→A, located in exon 2), was associated with recurrence-free survival. Patients with one or two copies of the minor (risk) allele had an increased risk of recurrence or death (hazard ratio [HR] 1.86, 95% CI 1.17–2.95; $p=0.0084$) in multivariate analysis. Median recurrence-free survival for carriers of the risk allele was 19 months (95% CI 9–not reached) versus 50 months (95% CI 37–75) for patients without the risk allele. In the validation cohort the HR was 2.45 (95% CI 1.01–5.95; $p=0.048$).

	Gene	Number assessable*	Minor allele frequency (%)	Homozygous (%)	Heterozygous (%)	Wild-type (%)	p value for HWE	p value for recurrence-free survival†	q value
Discovery cohort									
rs11762213 (G→A)	<i>MET</i>	393	5.3%	1.3%	8.1%	90.6%	0.0028	9.40×10^{-5}	0.027
rs3820546 (A→G)	<i>SLC2A1</i>	387	46.8%	23.8%	46.0%	30.2%	0.15	0.0019	0.27
rs38846 (T→C)	<i>MET</i>	389	18.6%	3.9%	29.6%	66.6%	0.62	0.0093	0.73
rs1531290 (A→G)	<i>KDR</i>	397	46.3%	22.4%	47.9%	29.7%	0.48	0.01	0.73
rs2236416 (A→G)	<i>MMP9</i>	398	13.8%	2.5%	22.6%	74.9%	0.29	0.023	0.89
rs38845 (G→A)	<i>MET</i>	390	45.5%	19.7%	51.5%	28.7%	0.48	0.029	0.89
rs1326889 (T→C)	<i>AGT</i>	362	48.3%	25.4%	45.9%	28.7%	0.12	0.031	0.89
rs3093662 (A→G)	<i>TNF</i>	386	8.2%	0.5%	15.3%	84.2%	1.00	0.032	0.89
rs361525 (G→A)	<i>TNF</i>	398	4.8%	0.3%	9.0%	90.7%	0.60	0.033	0.89
rs10267099 (A→G)	<i>ABCB1</i>	347	23.3%	6.3%	34.0%	59.7%	0.37	0.034	0.89
rs779805 (A→G)	<i>VHL</i>	399	32.3%	9.8%	45.1%	45.1%	0.57	0.035	0.89
rs10271561 (T→C)	<i>MET</i>	391	10.4%	0.8%	19.2%	80.1%	0.78	0.037	0.89
Validation cohort									
rs11762213 (G→A)	<i>MET</i>	148	5.4%	0%	10.8%	89.2%	1.00	0.042	..
rs3820546 (T→C)	<i>SLC2A1</i>	148	47.3%	21.6%	51.4%	27.0%	0.87	0.064	..

p value for HWE represents the exact test for HWE. Data are for the top 12 single nucleotide polymorphisms associated with recurrence-free survival in the discovery cohort and the top two in the validation cohort. HWE=Hardy-Weinberg equilibrium. *Patients whose genotyping had failed were excluded from the analysis. †For test of association between recurrence-free survival and single nucleotide polymorphism.

Table 3: Single nucleotide polymorphisms associated with recurrence-free survival



Children's Hospital
Informatics Program



Harvard
Medical School



Thank you for your attention